IEEE/CSC & ESAS European Superconductivity News Forum (ESNF), No. 14, October 2010
The published version of this manuscript appeared in *IEEE Transactions on Applied Superconductivity* **21**, Issue 3, 2036 - 2041 (2011)

Review of design aspects for high current Nb_3Sn conductors

Pierluigi Bruzzone

***Abstract*— Cabled conductors based on Nb_3Sn technology with operating current in the range of 20 kA and above are mainly restricted to fusion magnets and high field facilities. The experience of last decade has dramatically shown that, opposite to the NbTi conductors, straight scaling laws from the strands properties are not adequate for a reliable conductor design. Reversible and irreversible degradation heavily affects the conductor performance and frustrates the outstanding progress on the high current density Nb_3Sn strands. The evidence of performance degradation upon electromagnetic and thermal cycles is a further concern for a reliable and effective design. The knowledge to improve the design of Nb_3Sn high current conductors is gained in little steps, collecting over a longer period the results from different projects, including the test of short length conductors and model coils. This review highlights the key results from the last decade with the aim of drawing relevant conclusions about the impact of the individual layout and technology parameters on the performance degradation, including the strand technology, the cabling pattern, the void fraction, the aspect ratio, the electromagnetic load, the longitudinal strain and the magnet technology.**

***Index Terms*— Superconducting cables, Superconducting filaments and wires**

I. Introduction

HIGH current Nb_3Sn conductors are required in windings operating at high field with high stored energy, in order to limit the self-inductance and hence the voltage at current dump. The use of Nb_3Sn based conductors with operating currents in the range of 20 kA and above is presently restricted to fusion and large, high field magnets. In the field of accelerator magnets, prototypes of Nb_3Sn Rutherford cables are built with operating current up to 20 kA – however, this specific subject is not discussed in the present review.

In the last two decades, only Cable-in-Conduit Conductors (CICC) have been developed and manufactured for fusion and large high field magnets [1-3]. The manufacturing method was either wind-and-react (WR) or wind-react-transfer (WRT) technique. The last windings made of cabled Nb_3Sn strands according to the react-and-wind (RW) technique (T-15, SULTAN, DPC-EX) date over 20 years ago [4-6].

At large, the main advantages of the CICC over other conductor designs are the easy manufacture, by loose bundling of the desired number of Nb_3Sn strands, and the moderately low coupling currents loss, due to the high transverse resistance at the strand crossovers.

The main intrinsic drawbacks of the Nb_3Sn CICC are the large pressure drop, due to the very small hydraulic diameter of the strand bundle, the need of the WR technique, which requires that the electrical insulation withstand the heat treatment, the mismatch of the coefficient of thermal expansion of the conduit material and the Nb_3Sn strands and the low engineering current density. In some applications, layout modifications have been applied to mitigate the drawbacks, e.g. the "pressure release channel" and the insulation procedure WRT after heat treatment in the ITER conductors [7] and the Incoloy® conduit for the KSTAR conductors [8].

This review is restricted to the design aspects, which affect the electro-magnetic performance of Nb_3Sn CICC.

II. Performance Degradation Review

A. Strain sensitivity of free standing Nb_3Sn strands

Mechanical tension or compression applied to Nb_3Sn strand modifies the lattice parameters and hence affects the transport properties of the superconducting filaments. The behavior of the critical current density, J_c, versus longitudinal strain, ε, has been investigated and described since about 30 years [9]. A critical review of the various scaling laws for J_c vs. B, T, and ε can be found in [10]. Comparatively less attention was devoted to the effect of transverse compression [11-12].

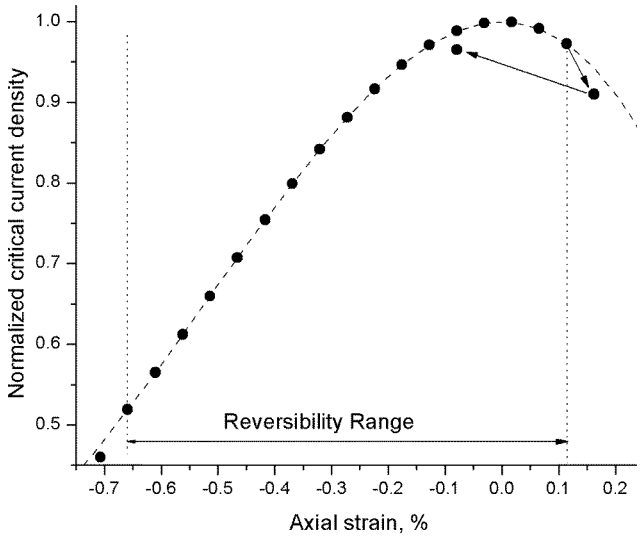

Figure 1 Typical $J_c(\varepsilon)$ curve of a high current density strand @12 T, 4 K.

Manuscript received 3 August 2010.

Pierluigi Bruzzone is with EPFL-CRPP, Fusion Technology, CH-5232 Villigen PSI, Switzerland (phone: +41 56 3104363; fax: +41 56 3103729; e-mail: pierluigi.bruzzone@psi.ch).

The reversibility window in a plot of $J_c(\varepsilon)$ is defined as the range of load/strain within which the J_c performance remains reversible, see Fig. 1. Recent studies [13, 14] have shown that the reversibility range is severely reduced in high current density strands, with very little tolerance to tensile load. In general, when the electric field criterion E_c is reduced from 100 μV/m (as it was in early data) to 10 μV/m, the apparent range of reversibility shrinks and cyclic load sensitivity is observed [14]. In some cases the reversibility window is restricted to the compressive strain, e.g. -0.6% to 0%. The most sensitive indicator of degradation is the n-index of transition assessed at low electric field.

The scaling laws for J_c are of empirical nature and use various sets of parameters to interpolate the test results. The conductor and coil designers must first identify a Nb_3Sn strand on the market, obtain the scaling parameters for that strand and then use the scaling laws in the design tools.

The scaling law parameters are drawn from test results within the range of reversibility and should only be used for "intact" strands within that range.

B. *The Nb_3Sn strain inside a CICC*

The Nb_3Sn filament axial strain has two components. The *thermal* strain, ε_{th}, is due to the mismatch of coefficient of thermal expansion among the CICC components from the heat treatment temperature to 4 K. For the Nb_3Sn filaments, $\varepsilon_{th} < 0$ (compression). The *operating* strain, ε_{op}, is the results of the electromagnetic forces on the winding. In most cases, ε_{op} is positive (tension) and partly relieves ε_{th}.

The prediction of the actual filament strain in a CICC is a major issue for the use of scaling laws in the conductors and windings design. The bundle of cabled strands in the conduit is not rigidly bonded. When a change of length is applied to the conduit, the axial strain is not directly transferred to the filaments, i.e. an assessment of the filament strain based on the "fully bonded" model ($\varepsilon_{th} < -0.85\%$ for CICC with steel conduit) tends to overestimate the actual strain. The effect of "settling" of the strands inside the conduit is dealt by introducing an empirical strain relaxation factor of the order of 30% on top of the strain obtained from the fully bonded model [7]. The settling effects depend on the local void fraction, cable pitches, friction at the strand crossovers and rigidity (layout) of the strands.

Measurements of $I_c(\varepsilon)$ on CICC were aimed to assess ε_{th} as the elongation applied to the CICC in order to achieve the peak performance, ε_{ap}. Typical values for ε_{ap} at peak performance are of the order of -0.65% for steel conduit [15]. However, the measured, applied strain on the conduit does not correspond to the actual strain transferred to the filaments inside the CICC, i.e. $\varepsilon_{th} < \varepsilon_{ap} < -0.65\%$.

Direct, in-situ measurements of the filament strain state in a CICC were attempted by neutron diffraction (measurement of the lattice parameter). So far, this method has not provided reliable results [16].

An experiment on going at CRPP is attempting to accurately measure the critical temperature as a function of the applied field, $T_c(B)$, in-situ in a CICC and compare with the $T_c(B, \varepsilon)$ data for a free standing strand to obtain ε_{th}.

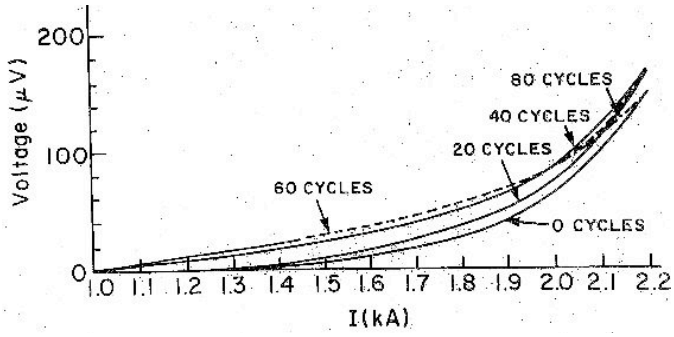

Figure 2. Broadening of the superconducting transition of a 27-strands, Nb_3Sn CICC as a function of the number of cycles. Milestone from 1985 [23].

C. *Early evidence of irreversible degradation in CICC*

Other attempts were made since one decade to deduce ε_{th} from the performance of CICC short samples, e.g. [17], and coil [18] using the scaling laws for the strand performance. This fitting procedure for ε_{th} implies that the Nb_3Sn strands in the CICC are still in the reversibility range. In fact, when results at various temperatures and fields are considered, a single ε_{th} value could not fit the full data set, i.e. the scaling law did not work. The analysts insisted on working on reversible performance. Complex "ad hoc" assumptions were retained to bridge the scaling laws with the actual performance. An "extra strain", depending on the operating load, was invoked e.g. in [18, 19] leading to non-realistic, extrapolated values of ε_{th}.

Another speculation to justify the early voltage and broad transition in conductors and coils made of Nb_3Sn CICC was a large unbalance of current distribution coupled with huge inter-strand resistance at the joint, preventing current re-distribution [20]. Eventually it was recognized that using realistic, measured values of contact and inter-strand resistance it is not possible to reproduce the behavior of Nb_3Sn CICC at transition [18, 21, 22].

The plain, incontrovertible evidence of irreversible degradation in Nb_3Sn CICC is the performance loss upon cyclic load. The first report about cyclic load degradation of Nb_3Sn CICC (broadening of the superconducting transition) dates back to 1985, see Fig. 2 from a PhD thesis at MIT [23]. Although other cases of performance mismatch were observed in the following years, LCT-WH [24] and DPC coils [25], it was only after the ITER CSMC test (2000) that the issue of irreversible degradation was brought to the attention of the community, Fig. 3 from [26].

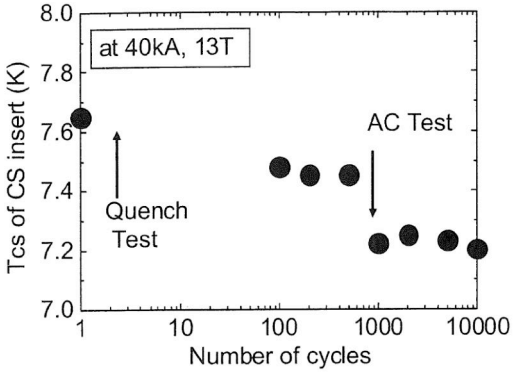

Figure 3. ITER CS Insert (2000): degradation of T_{cs} vs. number of cycles [26].

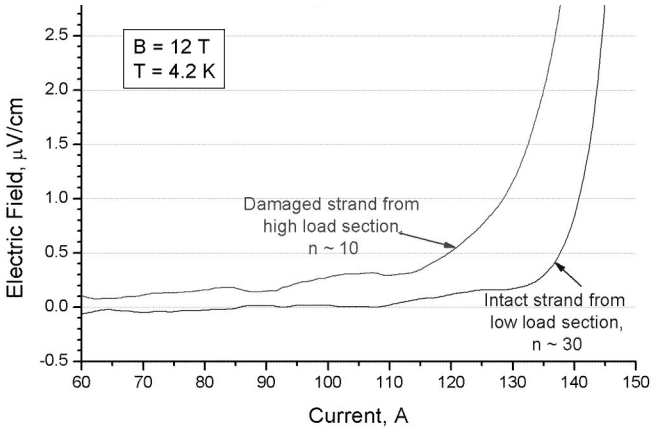

Figure 4. I_c test of Nb_3Sn strands extracted from sections of a CICC exposed to different electro-magnetic load (2002).

Starting from 2001, many results of cyclic load degradation on Nb_3Sn CICC were produced at the SULTAN facility on short samples [27-31]. In the meantime the test upon cyclic load is part of the qualification tests of the ITER conductors.

A crucial experiment to prove the irreversible degradation of Nb_3Sn strands in a CICC was done at CRPP in 2002 [32] by measuring the critical current on individual strands extracted from CICC previously exposed at high and respectively low electro-magnetic load, Fig. 4. At best, the irreversible degradation is quantified by the drop of the n-index. Because of the early voltage, the degradation reduces the operating range of a CICC. On the other hand, when the n-index decreases below 10, the temperature margin up to the take-off dramatically increases and the conductor is rock solid against large transient disturbance, as it was observed since 1999 [33].

Stimulated by the evidence of irreversible degradation, sophisticated metallographic techniques were developed in 2003 [34] to detect the filament cracks occurring under bending at the tensile edge, see Fig. 5. The role of strand bending in CICC under transverse load also received more attention from the analysts [35, 36], starting from the earlier work in [9]. However, the analysis remained confined to the reversibility range. As a matter of fact, reversible and irreversible degradation are linked together: the occurrence of cracks tends to relax the thermal and operating strain [16]. So far, no analytical, predictive model has been developed, which reliably includes the irreversible and cyclic load degradation.

D. Selected results from R&D on Nb_3Sn CICC

Even before applying cyclic load, the CICC performance could not be fitted by scaling law in the reversible range. The operation of the CMSC facility [37] and dedicated tests in the SULTAN facility [38] suggested that thermal cycles, from the first cool-down on, cause irreversible degradation comparable

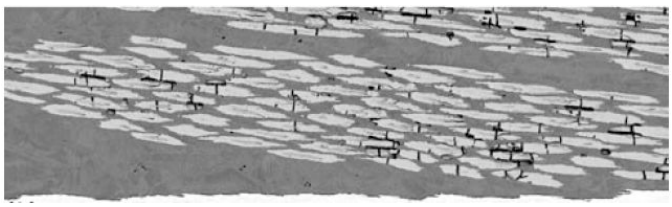

Figure 5. Filament cracks highlighted in a longitudinal section of a twisted strand upon bending, near the tensile edge [34] (2003).

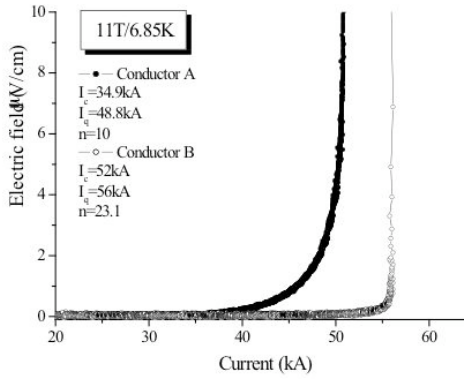

Figure 6. Performance of two identical, large CICC with solder filling (B) and with 35% void fraction [39] (2003).

to the load cycles. One additional warm-up/cool-down cycle is now part of the qualification tests of the ITER conductors.

Two similar experiments, where the cable space was impregnated respectively by solder [39] and resin/ice [40], proved that substantial damage occurs since the first cool down, with large degradation of both I_c and n-index, Fig. 6.

In an attempt to limit the strand bending under cool-down and transverse load, a low void fraction was identified by ITER as a CICC layout parameter to mitigate degradation. The design void fraction was reduced from originally 36% (1998) to 33% (2004) and eventually 30% (2007). A strict assessment of the void fraction impact on the performance of the ITER TF conductors can be drawn by the performance comparison of four samples where only the void fraction was the varying parameter. The results listed in Table I (from [30]) suggest that in the two bronze conductors "EAS" and "JAB" the reduced void fraction has no impact on the performance. For the internal Sn conductors "JAI" and "RF", a performance

TABLE I
FOUR SULTAN CONDUCTOR SAMPLES WITH IDENTICAL CABLES BUT DIFFERENT VOID FRACTIONS [30]

Conductor Nickname	EAS1/EAS2	JAB1/JAB2	JAI1/JAI2	RF33/RF30
Strand type	Bronze	Bronze	Int. Sn	Int. Sn
Void fraction, %	33.8/29.3	33.5/29.6	32.9/29.8	32.9/31.8
T_{cs} at 12 T, 68 kA, K	6.35 / 6.35	6.40 / 6.40	5.50 / 5.95	5.90 / 6.25

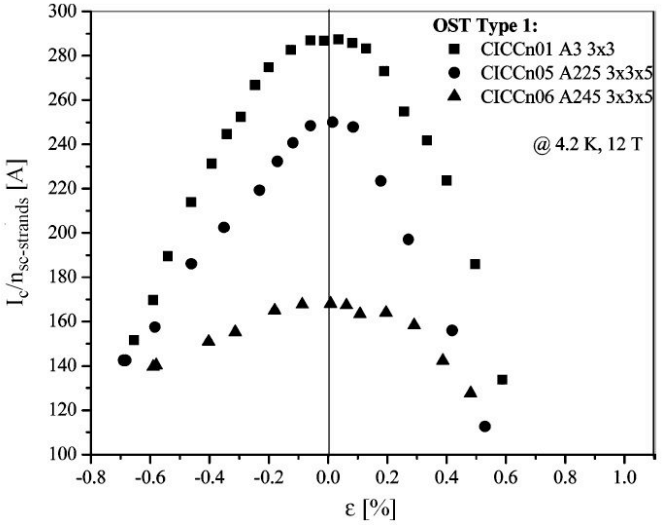

Figure 7. Performance of CICC with different void fraction [43]: triangles (45%), squares (32%), circles (25%).

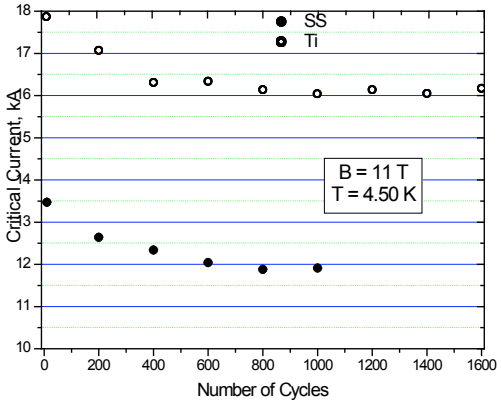

Figure 8. Critical current versus number of load cycles for CICC made of stainless steel and titanium jacket. The amount of irreversible performance degradation is similar despite the different thermal strain [28] (2004).

improvement is observed at lower void fraction. During the EDIPO conductor development, with high current density strand [31, 41], results from samples with different void fraction suggested a final conductor layout with ≈30% void fraction. A quantitative effect of the void fraction was hard to draw because other parameters in the samples were changed at the same time.

Other results on small size CICC as a function of the void fraction [42] show higher performance at 30% compared to 36% void. In Fig. 7, from [43], the optimum performance is achieved at 32% void – the CICC with 25% void is inferior, likely due to cable damage at the extreme compaction.

In 2004, two CICC with identical cable and void fraction but different conduit material were tested in SULTAN for cyclic load degradation [28]. Some analysts expected that the CICC with steel conduit could better withstand the transverse load because the strands can bend without entering the dangerous tensile region thanks to the higher thermal compressive strain. The results for stainless steel and titanium conduit, Fig. 8, actually show a similar amount of irreversible degradation relative to the initial performance, despite the different thermal strain.

The cable pattern is the layout parameter that received most attention in the recent R&D for ITER conductors. The cable configuration, e.g. "triplet", "1+6", braid, and the sequence of

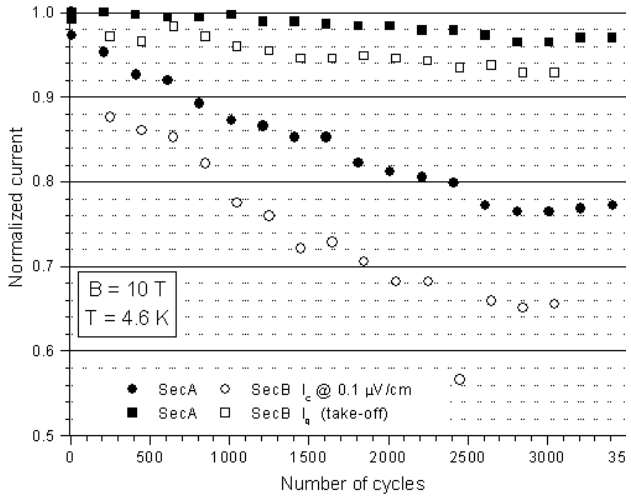

Figure 9. Critical current vs. number of load cycles for CICC based on triplet (SecA) and 1+7 cable layout (SecB) [27].

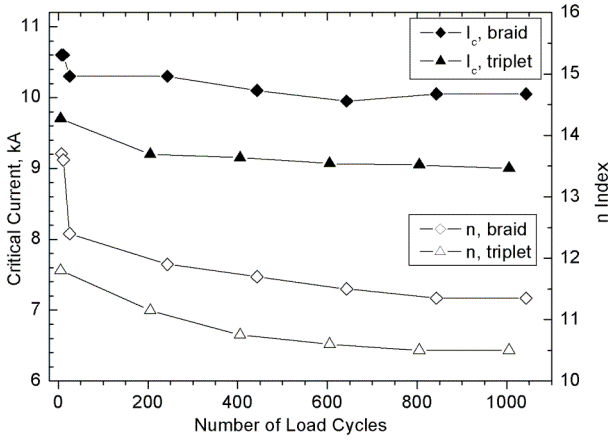

Figure 10. Performance of two CICC made of braided and tripleted based cables respectively [29].

cable pitches in the multi-stage cable, affect the transverse modulus of the cable and the loading pattern in operation. A comparison between the "triplet" and "1+7" pattern [27] suggested less degradation for the triplet, Fig. 9. Later investigations on the subject, with more layout variations, confirmed this qualitative trend [42]. The braided pattern turns out to be superior to the triplet, likely due to the higher transverse modulus [29], Fig. 10.

For CICC made of triplet based cables, the issue of "long" vs. "short" pitch sequence was addressed both by models [44] and R&D on small [43, 42] and large [45] CICC. A crucial experiment is reported in [46], where two sequences of cable pitches are realized on one section of cable and tested in the same sample in SULTAN, Fig. 11. The effectiveness of the "long" pitch sequence to reduce the irreversible degradation is clear both as T_{cs} performance and n-index. The thermal strain ε_{th} fitting the results of the ITER prototype conductor TFPRO2-OST2, made with long cable pitches, was as small as -0.46% [45], implying that when "fitting" ε_{th} in the range of -0.6% to -0.7% are drawn in similar CICC, a large irreversible degradation is actually present.

For a conductor carrying current in a background magnetic field, the distribution of electromagnetic load and magnetic field have peaks at opposite sides. For Nb_3Sn CICC, the

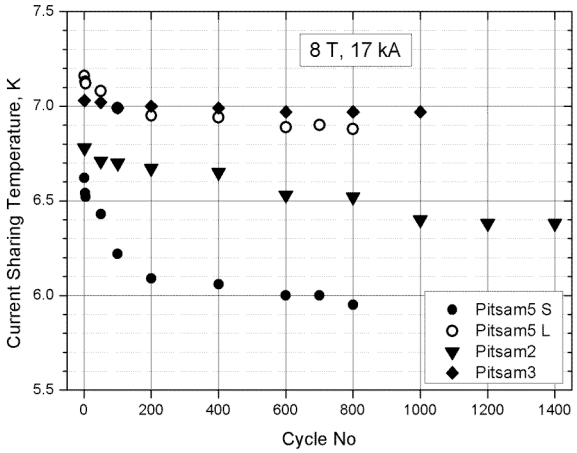

Figure 11. Performance of CICC with layout variations: round cables with short (full circles), medium (triangles) and long (open circles) pitches vs. a rectangular cable (aspect ratio = 1.7) with medium pitches (diamonds) [46].

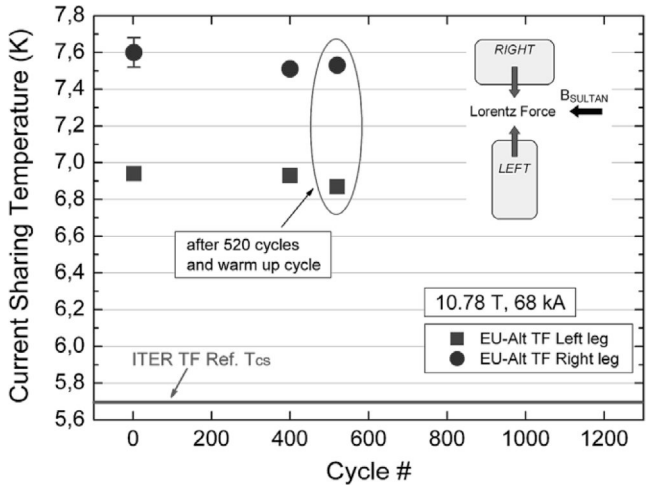

Figure 12. Performance of a large rectangular CICC with an aspect ratio of 2 in both orientations with respect to the background field [49]

transition occurs at the low field side, as the mechanical degradation dominates the transport properties [36]. A cable with rectangular cross section, with broad side parallel to the background field, has a lower peak load compared to a round cable at the same *BI* product. Flat cables are expected to minimize the performance degradation due to operating loads. In fact, R&W conductors, where the flat cable choice is mandatory to allow a broad range of bending during the coil manufacture, show high n-index and high performance even at moderately high void fraction and "short" pitches [47, 48].

The impact of cable shape and pitches for the EDIPO LF conductor is summarized in Fig. 11 [46]. The mitigation of degradation using a rectangular cable is better than using long cable pitches. The EDIPO [2] and the SCH [3] projects use rectangular CICC for the high field conductor with aspect ratio of 2.6 and 2.35 respectively. Both conductors have been tested in SULTAN with limited degradation.

A crucial experiment is reported in [49]. A rectangular CICC with an aspect ratio of 2 is tested in SULTAN in both orientations with respect to the background field, i.e. with peak load at the edge of the long and short side respectively.

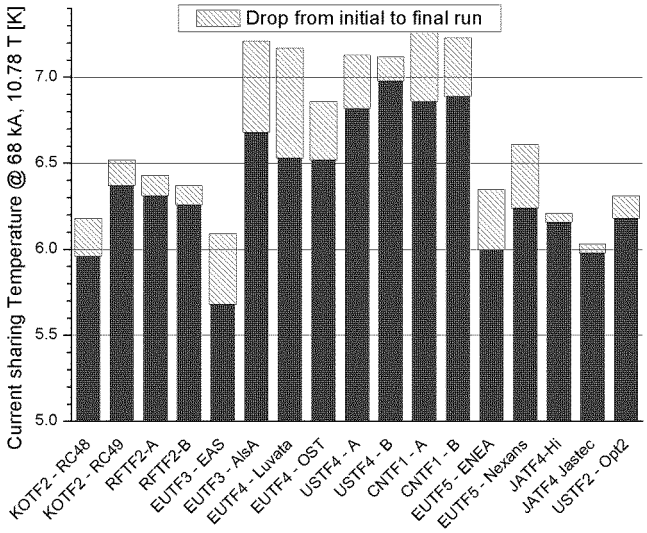

Figure 13. Initial and final performance of the ITER TF conductor samples built to the same specification (Option2) from different Nb_3Sn strands [50, 51, 52].

At the same operating field and current, the ratio of the peak load is 4. The results in Fig. 12 stress the role of the aspect ratio in mitigating the irreversible degradation.

The issue of cyclic load degradation in ITER TF conductors was reviewed in [50-52] for the qualification samples. The plot in Fig. 13 shows the initial and final performance for a number of ITER conductor samples prepared according the "Option2" cable layout, i.e. long cable pitch sequence and 30% void fraction. Except the strand type, the CICC are identical. The variability of the performance and its evolution is dominated by the layout (robustness) of the strand. The smallest performance drop with cyclic load is with the JATF4 and the largest with EUTF4. The strand layout, i.e. the width of its window of reversibility, is the key parameter, which affects the CICC performance at most.

III. The Designer Perspective

The R&D results listed above show design trends to mitigate the CICC degradation. A *low void fraction* is either neutral or beneficial in term of DC performance, but it enhances the AC loss and the hydraulic pressure drop. This last issue can be solved by a *pressure release channel*, which on the other hand weakens the transverse modulus and allows large cable displacements under electromagnetic loads. Very *high J_c in the strand* improves the DC margin, but tends to reduce the reversibility window. *Long cable pitches* are beneficial for strand bending inside the CICC at the price of higher AC loss and difficult/slow manufacture [53].

For a project starting from the scratch, the designer may have more ambitious goals than "mitigation of degradation" and include in his options also "non-CICC" conductors.

The good results with rectangular cables relaunch the R&W option [47-48]. In fact a flat cable tolerates bending and re-straightening after the heat treatment. With the conduit applied after the heat treatment, the thermal strain is drastically reduced and the performance of the free-standing strand becomes fully available in the conductor, with substantial cost impact on a large coil. The solder filling option has a good "demonstration" value, but it is not mandatory for a high performance conductor.

A radical option to avoid degradation would be to switch from Nb_3Sn to Nb_3Al, which is much more tolerant to strain [35]. However, J_c in intact strands is substantially higher for Nb_3Sn and the price of Nb_3Al remains today a major issue.

For most large Nb_3Sn CICC, the irreversible degradation causes a performance drop in the range of 20%-50% even after applying the "mitigating" measures. Despite attempts to either artificially enhance the reversible filament strain [19] or invoke an "area reduction" for the irreversible degradation in analysis of test results [29], no reliable, *predictive* tool that includes the irreversible degradation is available today for the designer. It is unlikely that such a universal tool, applicable to any strand, will be developed, because the amount of irreversible degradation and its evolution with thermal and electro-magnetic cycles depends mainly on the layout of the individual strands. The mandatory, non-effective, approach is to impose initially an over-generous design margin (using "reversible" tools) and adjust it underway, when test results

from prototypes become available.

Due to the limited number of projects in the area of high current, high field superconductors and to the lack of a continuous (expensive) R&D activity, the progress toward an effective conductor design is slow. The typical market feedback for a product and cost optimization is definitely not present for large superconductors.

REFERENCES

[1] P. Bruzzone, "30 Years of conductors for fusion. A summary and perspectives", IEEE Trans Appl. Supercon. 16, 839-844 (2006).

[2] A. Portone, et al., "Status of the EDIPO project", IEEE Appl. Supercond. 19, 1552-1555, (2009).

[3] I.R. Dixon et al., "Current Sharing and AC Loss Measurements of Cable-in-Conduit Conductor with Nb3Sn Strands for the High Field Section of the Series-Connected Hybrid Outsert Coil", IEEE Appl. Supercond. 19, 2466-2469 (2009).

[4] E. N. Bondarchuk et al., "Tokamak-15 electromagnetic system. Design and test results", Plasma Device and Operation, 2, 1 (1992).

[5] B. Blau et al., "First performance test of the 12 T split coil test facility SULTAN III", IEEE Trans Appl. Supercon. 3, 361-364 (1993).

[6] T. Ando et al., "Fabrication and test of the Nb_3Sn demo poloidal coil (DPC-EX)", Fusion Technology 1990, 243-246 (Elsevier 1991).

[7] ITER Final Design Report 2001: DRG1 Annex "Magnet Superconducting and electrical Design Criteria", IAEA Vienna 2001.

[8] K. Kim et al., "Status of the KSTAR superconducting magnet system development", Nuclear Fusion 45, 783 (2005).

[9] J.W. Ekin, "Strain scaling law and the prediction of uniaxial and bending strain effects in multifilamentary superconductors" in *Fialmentary A15 superconductors*, Plenum Press 1980, 187-203.

[10] L. Bottura, B. Bordini "$J_c(B, T, \varepsilon)$ parametrization for the ITER Nb_3Sn strands", IEEE Appl. Supercond. 19, 1521-1534 (2009).

[11] J.W. Ekin, "Effect of transverse compressive stress on the critical current and upper critical field of Nb_3Sn ", J. Appl. Phys. 62, pp. 4829, 1987.

[12] W. Specking, W. Goldacker and R. Flükiger, "Effect of transverse compression on I_c of Nb_3Sn multifilamentary wire", Adv. Cryo. Eng. 34, pp. 569, 1987.

[13] X.F. Lu, D.M.J. Taylor, S. Pragnell and D.P. Hampshire, "Extended strand characterisation", www.dur.ac.uk/superconductivity.durham/publications.html

[14] A. Nijhuis, Y. Ilyin, H.J.G. Krooshoop, W. Abbas, W.A.J. Wessel, "Extended strand characterization", Final Report UT-EFDA 2007-3.

[15] W. Specking et al., "The effect of cyclic axial strain on critical current of Cable-in-conduit NET subcables", IEEE Mag 27, 1825 (1991).

[16] P. Bruzzone, R. Wesche, F. Cau, "Results of thermal strain and conductor elongation upon heat treatment for Nb_3Sn Cable-in-Conduit Conductors", IEEE Appl. Supercond. 20, 470-473 (2010).

[17] D. Ciazynki et al., "Test results and analysis of two European full size conductors samples for ITER", IEEE Appl. Supercon. 10, 1058 (2000).

[18] N. Mitchell, "Summary, assessment and implications of the ITER model coil test results", Fusion Engineering and Design 66-68, 971-993 (2003).

[19] D. Ciazynski, Review of Nb_3Sn conductors for ITER", Fusion Engineering and Design, 82, 2007, 488-497.

[20] N. Mitchell, "Possible causes of the premature voltage gradient of the CS insert coil", IEEE Appl. Supercond. 12, 1453-1458 (2002).

[21] E.P.A. van Lanen et al., "Interstrand Resistance Measurements on the Conductor Terminations of TFPRO2 and JATF3 SULTAN Samples", IEEE Appl. Supercond. 20, 474-477 (2010).

[22] F. Cau, P. Bruzzone, M. Calvi, "Interstrand resistance and contact resistance distribution on terminations of ITER short samples", IEEE Appl. Supercond. 20, 478-481 (2010).

[23] P. Rezza, "Mechanical and electrical performance of superconducting cables subject to cyclic stress," MS at MIT, September 1985.

[24] The IEA Large Coil Task, Fusion Engineering and Design 7, 1&2, (1988).

[25] H. Tsuji et al., "Evolution of the Demo Poloidal Coil Program", Proc. 11th Conf on Magn. Tech., Essex, UK, 806 (1990).

[26] H. Tsuji et al., "ITER R&D: Magnets: Central Solenoid Model Coil", Fusion Engineering and Design 55, 153-170 (2001).

[27] P. Bruzzone, A. Fuchs, B. Stepanov, G. Vecsey, "Performance evolution of Nb_3Sn Cable-in-Conduit Conductors under cyclic load", IEEE Appl Supercond 12, 516-519 (2002).

[28] N. Martovetsky et al., "Effect of the conduit material on CICC performance under high cycling loads", IEEE Trans Appl. Supercon. 15, 1367-1370 (2005).

[29] P. Bruzzone, B. Stepanov, R. Wesche, "Transverse load degradation in Nb_3Sn Cable-in-conduit Conductors with different cable pattern", Adv. Cryog. Eng. 52 B, 558-565 (2006).

[30] P. Bruzzone et al. , "Results of a new generation of ITER TF conductor samples in SULTAN", IEEE Appl. Supercond. 18, 459-462, (2008).

[31] A. Vostner et al., "Development of the EFDA dipole high field conductor", IEEE Appl. Supercond. 18, 544-547, (2008).

[32] P. Bruzzone, R. Wesche, B. Stepanov, "The voltage current characteristic (n value) of the cable-in-conduit conductors for fusion", IEEE Appl Supercond 13, 1452 (2003).

[33] P. Bruzzone, "Stability under transverse field pulse of the Nb3Sn ITER cable-in-conduit conductors", IEEE Appl Supercond 10, 1062 (2000).

[34] M.C. Jewell, P.J. Lee, D.C. Larbalestier, "The influence of Nb_3Sn strand geometry on filament breakage under bend strain as revealed by metallography", Supercond. Sci. Technol. 16 (2003) 1005–1011.

[35] N. Mitchell, "Analysis of the effect of Nb3Sn strand bending on the CICC superconductor performance", Cryogenics 42 (2002) 311-325.

[36] N. Koizumi, Y. Nunoya, K. Okuno, "A new model to simulate critical current degradation of large CICC by taking into account strand bending", IEEE Appl. Supercond. 16, 831-834, (2006).

[37] R. Zanino et al., "EU contribution to the test and analysis of the ITER poloidal field conductor insert and the central solenoid model coil", Supercond. Sci. Technol. 22 (2009) 085006.

[38] P. Bruzzone et al., "Test Results of two ITER TF conductor short samples using high current density Nb_3Sn strands", IEEE Appl. Supercond. 17, 1370-1373, (2007).

[39] G. Pasztor, P. Bruzzone, A. Anghel, B. Stepanov, "An alternative CICC design aimed at understanding critical performance issues in Nb_3Sn conductors for ITER", IEEE Appl. Supercond. 14, 1527-1530 (2004).

[40] K. Seo et al., "Mitigation of critical current degradation in mechanically loaded Nb_3Sn superconducting multi-strand cable", IEEE Appl. Supercond. 18, 491-494 (2004).

[41] Manufacturing of subsize cable-in-conduit conductors, CRPP Final Report to EFDA contract 06-1479, TW6-TMSC-PITSAM, Nov. 2007.

[42] I.R. Dixon et al., "Electromagnetic cycling and strain effects on Nb_3Sn cable-in-conduit conductors with variations of cabling design and conduit material properties", IEEE Appl. Supercond. 19, 1462-1465, (2009).

[43] K.P. Weiss et al., "Systematic approach to examine the strain effect on the critical current of Nb_3Sn cable-in-conduit conductors", IEEE Appl. Supercond. 17, 1469-1472, (2007).

[44] A. Nijhuis, Y. Ilyin, "Transverse load optimization in Nb_3Sn design; influence of cabling, void fraction and strand stiffness", Supercond. Sci. Technol. 19 (2006) 945-962.

[45] D. Ciazynki et al., " Influence of Cable Layout on the Performance of ITER-type Nb_3Sn Conductors", Journal of Physics: Conference Series 97 (2008) 012027.

[46] P. Bruzzone et al., "Test results of a Nb_3Sn Cable-in-conduit Conductor with variable pitch sequence", IEEE Appl. Supercond. 19, 1448-1451 (2009).

[47] T. Ando et al., "The second test results on the Nb_3Sn demo poloidal coil (DPC-EX)", Adv. Cryog. Eng. 39, 335-341 (1994).

[48] P. Bruzzone et al., "Development of a react and wind conductor for the ITER toroidial field coils", IEEE Appl. Supercond. 18, 467-470, (2008).

[49] A della Corte et al., "Successful performances of the EU-AltTF sample, a large size Nb_3Sn cable-in-conduit conductor with rectangular geometry", 2010 Supercond. Sci. Technol. 23 045028.

[50] P. Bruzzone, B. Stepanov, R. Wesche, "Qualification tests for ITER TF conductors in SULTAN", Fusion Engineering and Design, 84, 2009, 205-209.

[51] P. Bruzzone et al. "Status Report of the SULTAN Test Facility", IEEE Appl. Supercond. 20, 455-457 (2010).

[52] P. Bruzzone et al. "Operation and test results from the SULTAN Test Facility", presented at ASC 2010, Washington August 2010.

[53] A. Di Zenobio et al. "Conductor manufacturing of the ITER TF full-size performance samples", IEEE Appl. Supercond. 20, 1412-1415 (2010).